Vol 17 No 9, September 2008
1674-1056/2008/17(09)/3471-08

Chinese Physics B

© 2008 Chin. Phys. Soc.
and IOP Publishing Ltd

Self-organized GaN/AlN hexagonal quantum-dots: strain distribution and electronic structure*

Liu Yu-Min(刘玉敏)[a)b)†], Yu Zhong-Yuan(俞重远)[a)b)],
Ren Xiao-Min(任晓敏)[b)], and Xu Zi-Huan(徐子欢)[a)b)]

[a)] *School of Science, Beijing University of Posts and Telecommunications, Beijing* 100876, *China*
[b)] *Key Laboratory of Optical Communication and Lightwave Technologies of Ministry of Education (Beijing University of Posts and Telecommunications), Beijing* 100876, *China*

(Received 3 March 2008; revised manuscript received 30 March 2008)

This paper presents a finite element method of calculating strain distributions in and around the self-organized GaN/AlN hexagonal quantum dots. The model is based on the continuum elastic theory, which is capable of treating a quantum dot with an arbitrary shape. A truncated hexagonal pyramid shaped quantum dot is adopted in this paper. The electronic energy levels of the GaN/AlN system are calculated by solving a three-dimension effective mass Shrödinger equation including a strain modified confinement potential and polarization effects. The calculations support the previous results published in the literature.

Keywords: quantum dot, strain, electronic structure
PACC: 7320D, 0365, 4620

1. Introduction

Progress in semiconductor growth technology has made it possible to fabricate self-organized quantum dot (QD) materials, which are the ultimate limit for carrier confinement. Their atom-like density-of-state (DOS) provides potential applications in opto-electronic and microelectronic devices.[1] It has been demonstrated that the shape and the area densities of the quantum dots can be controlled by varying the growth parameters such as the growth temperature, the growth rate, the annealing progress and the growth interruptions. In the early studies about the calculations of quantum dot electronic structures, the strain are often taken to be a constant in the quantum and zero in the surrounding barriers, while the quantum dot is often simplified into a cube or cylinder in shapes.[2,3] In this paper we employ a more realistic truncated hexagonal pyramid shaped GaN/AlN quantum dot in calculating the electronic structures. The strain effect and the piezoelectric effect are also taken into account. We use the continuum elastic theory to determine strain distributions. The effect of strain on the electronic energy levels is calculated by the eight-band $\boldsymbol{k}\cdot\boldsymbol{p}$ theory. The piezoelectric effect is taken into consideration by introducing a piezoelectric potential in the Schrödinger equation.

2. Strain distributions

For convenience, the dependence of strain components on stress components can be set up by using a stiffness matrix $\boldsymbol{D}$, and then the strain and the stress may be expressed as two column vectors[4]

$$\boldsymbol{\varepsilon} = \begin{pmatrix} \varepsilon_{xx} \\ \varepsilon_{yy} \\ \varepsilon_{zz} \\ \varepsilon_{xy} \\ \varepsilon_{yz} \\ \varepsilon_{zx} \end{pmatrix} = \begin{pmatrix} \partial u/\partial x \\ \partial v/\partial y \\ \partial w/\partial z \\ (\partial u/\partial y + \partial v/\partial x)/2 \\ (\partial v/\partial z + \partial w/\partial y)/2 \\ (\partial u/\partial z + \partial w/\partial x)/2 \end{pmatrix}, \tag{1a}$$

and

$$\boldsymbol{\sigma} = \begin{pmatrix} \sigma_{xx} \\ \sigma_{yy} \\ \sigma_{zz} \\ \sigma_{xy} \\ \sigma_{yz} \\ \sigma_{xz} \end{pmatrix} = \boldsymbol{D}(\boldsymbol{\varepsilon} - \varepsilon_0) + \sigma_0, \tag{1b}$$

*Project supported by the State Key Development Program for Basic Research of China (Grant No 2003CB314901), the National Natural Science Foundation of China (Grant No 60644004), and High School Innovation and Introducing Intellect Project of China (Grant No B07005).
†E-mail: liuyuminhqy@263.net

where u, v and w are the displacements along the coordinates x, y and z directions respectively. For the cubic crystal the $\boldsymbol{D}$ matrix can be expressed as

$$\boldsymbol{D} = \begin{bmatrix} C_{11} & C_{12} & C_{13} & 0 & 0 & 0 \\ C_{12} & C_{11} & C_{13} & 0 & 0 & 0 \\ C_{13} & C_{13} & C_{33} & 0 & 0 & 0 \\ 0 & 0 & 0 & \dfrac{(C_{11}-C_{12})}{2} & 0 & 0 \\ 0 & 0 & 0 & 0 & C_{44} & 0 \\ 0 & 0 & 0 & 0 & 0 & C_{44} \end{bmatrix}. \quad (2)$$

As can be seen, there exist three independent elastic constants. The lattice constants in a quantum dot system vary with coordinate, therefore the elastic energy can be expressed as an integral expression

$$U = \frac{1}{2}\int C_{ijkl}\left(\varepsilon_{ij} - \varepsilon^0_{ij}\delta_{ij}\right)\left(\varepsilon_{kl} - \varepsilon^0_{kl}\delta_{kl}\right)\mathrm{d}v. \quad (3)$$

The components of ε^0_{ij} are the initial strain in the quantum dot system. In a quantum dot region, the initial strain is the lattice mismatch of the heterostructure materials. In the surrounding barriers, the initial strain is zero. The lattice mismatch can be expressed as

$$\varepsilon^0_{i,j} = \begin{cases} \varepsilon^0_{xx} = \varepsilon^0_{yy} = \dfrac{a_{\mathrm{dot}} - a_{\mathrm{sub}}}{a_{\mathrm{sub}}} - 0.024, \\ \varepsilon^0_{zz} = \dfrac{c_{\mathrm{dot}} - c_{\mathrm{sub}}}{c_{\mathrm{sub}}} = -0.039, \\ \varepsilon^0_{i,j} = 0 \quad i \neq j. \end{cases} \quad (4)$$

Substituting expressions (4) and (1) into expression (3), the elastic strain energy of the quantum dot system can be expressed as

$$\begin{aligned} U = \frac{1}{2}\iiint \Big\{ & C_{11}\left(\varepsilon^2_{xx} + \varepsilon^2_{yy}\right) + C_{33}\varepsilon^2_{zz} + 2C_{12}\varepsilon_{xx}\varepsilon_{yy} + 2C_{13}\varepsilon_{zz}\left(\varepsilon_{xx} + \varepsilon_{yy}\right) \\ & + 4C_{44}\left(\varepsilon^2_{yz} + \varepsilon^2_{xz}\right) + 2\left(C_{11} - C_{12}\right)\varepsilon^2_{xy} - 2\varepsilon^0_{xx}\left(C_{11} + C_{12}\right)\left(\varepsilon_{xx} + \varepsilon_{yy}\right) \\ & - 2C_{33}\varepsilon_{zz}\varepsilon^0_{zz} - 2C_{13}\left[2\varepsilon_{zz}\varepsilon^0_{xx} + \varepsilon^0_{zz}\left(\varepsilon_{xx} + \varepsilon_{yy}\right)\right] \\ & + 2C_{11}\left(\varepsilon^0_{xx}\right)^2 + C_{33}\left(\varepsilon^0_{zz}\right)^2 + 2\varepsilon^0_{xx}\left(C_{12}\varepsilon^0_{xx} + 2C_{13}\varepsilon^0_{zz}\right)\Big\}\mathrm{d}v. \end{aligned} \quad (5)$$

3. Piezoelectric effects

Under an applied stress, a semiconductor will develop an electric moment. The magnitude of electric moment is proportional to the stress. The strain induced polarization P can be related to the strain tensor by using the piezoelectric coefficients e_{ilm} as follows:

$$P^{\mathrm{strain}}_i = \sum_{lm} e_{ilm}(r)\varepsilon_{lm}(r). \quad (6)$$

In the common matrix representation it is written as

$$\begin{pmatrix} P^{\mathrm{strain}}_x \\ P^{\mathrm{strain}}_y \\ P^{\mathrm{mstrain}}_z \end{pmatrix} = \begin{pmatrix} e_{11} & e_{12} & e_{13} & e_{14} & e_{15} & e_{16} \\ e_{21} & e_{22} & e_{23} & e_{24} & e_{25} & e_{26} \\ e_{31} & e_{32} & e_{33} & e_{34} & e_{35} & e_{36} \end{pmatrix} \begin{pmatrix} \varepsilon_{xx} \\ \varepsilon_{yy} \\ \varepsilon_{zz} \\ 2\varepsilon_{yz} \\ 2\varepsilon_{zx} \\ 2\varepsilon_{xy} \end{pmatrix}. \quad (7)$$

For a crystal structure with an inversion symmetry $P = -P$, $e_{ij} \equiv 0$, for all i, j. For a GaN/AlN crystal with a wurtzite structure, all components of e_{ij} are zero expect $e_{31} = e_{32}$, e_{33}, and $e_{24} = e_{15}$. As can be seen from Eq.(7), both the diagonal and off-diagonal terms of the strain tensor generate a built-in polarization field in the quantum dot. Wurtzite nitrides also exhibit a strong spontaneous polarization, P^{spont}, with polarity specified by the terminating anion or cation at the surface. So the total polarization can be expressed as

$$\boldsymbol{P}^{\mathrm{total}} = \boldsymbol{P}^{\mathrm{strain}} + \boldsymbol{P}^{\mathrm{spont}}. \quad (8)$$

Since the growth direction is along the c axis (z axis in Cartesian coordinates) for GaN/AlN quantum dots, the spontaneous polarization includes only the z component. The fixed piezoelectric charge density is obtained from the divergence of the polarization as

$$\rho(r) = -\nabla \cdot \boldsymbol{P}^{\mathrm{total}}(r). \quad (9)$$

In the absence of external charges, the piezoelectric potential V_{p} can be obtained by solving the Poisson

equation

$$\varepsilon_0 \nabla \cdot (\boldsymbol{\varepsilon}_r(r) \nabla V_{\mathrm{p}}) = \rho, \tag{10}$$

where $\boldsymbol{\varepsilon}_0$ and $\boldsymbol{\varepsilon}_{\mathrm{r}}$ are the dielectric constant in vacuum and the relative static dielectric tensor respectively. For the GaN/AlN material the dielectric tensor has the following form:

$$\boldsymbol{\varepsilon}_{\mathrm{r}} = \begin{pmatrix} \varepsilon^{\perp} & 0 & 0 \\ 0 & \varepsilon^{\perp} & 0 \\ 0 & 0 & \varepsilon^{//} \end{pmatrix}. \tag{11}$$

4. Electronic structure

The electronic structure is calculated in the single band envelope approximation with the modified band edge from the eight band $\boldsymbol{k} \cdot \boldsymbol{p}$ theory. The electron Hamiltonian is[5]

$$H_{\mathrm{e}} = -\frac{\hbar^2}{2m_{\mathrm{e}}^*}\nabla^2 + E_{\mathrm{c}} + \delta E_{\mathrm{c}} - eV_{\mathrm{p}}, \tag{12}$$

where E_{c} is the local conduction-band edge in the absence of strain; δE_{c} is the strain modified conduction-band edge that can be expressed as

$$\delta E_{\mathrm{c}} = a_{\mathrm{c}}^{\perp}\varepsilon_{\mathrm{hyd}}^{\perp} + a_{\mathrm{c}}^{//}\varepsilon_{\mathrm{hyd}}^{//} \tag{13}$$

with $a_{\mathrm{c}}^{\perp}$ and $a_{\mathrm{c}}^{//}$ being the conduction band deformation potentials, $\varepsilon_{\mathrm{hyd}}^{\perp} = \varepsilon_{xx} + \varepsilon_{yy}$ and $\varepsilon_{\mathrm{hyd}}^{//} = \varepsilon_{zz}$, where the subindex 'hyd' means the hydrostatic strain; e is the charge of one electron; and $\boldsymbol{m}_{\mathrm{e}}^*$ is the effective mass tensor of the electron and expressed as

$$\boldsymbol{m}_{\mathrm{e}}^* = \begin{pmatrix} m_{\mathrm{e}}^{\perp} & 0 & 0 \\ 0 & m_{\mathrm{e}}^{\perp} & 0 \\ 0 & 0 & m_{\mathrm{e}}^{//} \end{pmatrix}. \tag{14}$$

As can be seen from expression (11), the electron Hamiltonian includes the effect of strain modified conduction band edge, and piezoelectric potential energy. The values used for all kinds of material parameters are given in Table 1.[6]

Table 1. Material parameters of GaN/AlN used for calculations.

	$m_{\mathrm{e}}^{//}$	$m_{\mathrm{e}}^{\perp}$	C_{11}	C_{12}	C_{44}	C_{13}	C_{33}	e_{15}	e_{31}	e_{33}
GaN	0.2	0.2	390	145	105	106	398	–0.49	–0.49	0.73
AlN	0.28	0.32	396	137	116	108	373	–0.6	–0.6	1.46
	P^{spont}	$\varepsilon^{\perp}$	$\varepsilon^{//}$	E_{g}	E_{v}	E_{c}	$a_{\mathrm{c}}^{//}$	$a_{\mathrm{c}}^{\perp}$	a	c
GaN	–0.029	9.28	10.01	3.475	0	3.475	–9.5	–8.2	3.189	5.185
AlN	–0.081	8.67	8.57	6.23	–0.8	5.43	–5.4	1.16	3.112	4.982

5. Numerical calculations

In this paper we use the finite element method to calculate the strain energy. In the framework of thermoelasticity, to simulate initial strain, the thermal expansion coefficients of the GaN QD and wetting layer are introduced to be the absolute values of lattice mismatch which are $0.024\,\mathrm{K}^{-1}$ along the horizontal direction and 0.039 along the growth direction. The thermal expansion coefficient of AlN is zero. Then the initial strain of the system can be simulated by raising the temperature from a reference temperature 0 K to the strain temperature 1 K. The values of the reference temperature and strain temperature are only of relative significance. But the difference between the strain temperature and the reference temperature should be 1 K. Then the initial strain can be substituted by the effect of thermal expansion process.[4,7–9] The thermal expansion simulation environment is easy to realize by using the commercial finite element tools such as ANSYS. Using the ANSYS simulation environment, the elastic energy is minimized by using the conjugate gradient algorithm. When the system elastic energy arrives at a minimum value, the lattices are stable via relaxation. The boundary conditions are as follows: the four side faces are fixed along the direction normal to the side faces, the bottom side is fixed along the normal direction, the upper surface is free in all directions. Although the quantum dot is on nanometer scale, the strain distribution calculated by using the finite element method is reliable. A comparison has been made between the finite element method and more accurate atomic based method,[10] and the results show that only a little difference can be found near the boundary of the quantum dot.

Once the strain distribution is calculated by using the finite element method, the piezoelectric charge density and the piezoelectric potential can be eas-

ily calculated from Eqs.(9) and (10) directly by using the finite difference method to solve the Poisson equation. The electronic energy levels and eigenfunctions are also calculated by using the finite difference method.[11] The whole simulation region is discretized into N_x, N_y and N_z grids along the x, y and z directions. Then the discretized Eq.(12) using finite difference style is transformed into

$$H_{N\times N}\begin{pmatrix}\phi_1\\ \vdots\\ \phi_N\end{pmatrix} = E_{\rm n}\begin{pmatrix}\phi_1\\ \vdots\\ \phi_N\end{pmatrix}, \qquad (15)$$

where $H_{N\times N}$is a sparse square matrix; $N = N_xN_yN_z$ is the total number of the discretized points; $E_{\rm n}$ is the electronic energy level, which can be calculated by the Matlab software through solving the eigenvalue of the sparse matrix $H_{N\times N}$, of which the eigenvectors are the corresponding wavefunction of the electronic energy level $E_{\rm n}$.

6. Results and discussion

We consider a truncated hexagonal pyramid shaped GaN quantum dot on AlN, as has been observed for self-organized quantum dots growing experiments by using the molecular-beam epitaxy[12] technology. The thickness of wetting layer is 1 nm, the height of the quantum dot is 4 nm, the diameter of the bottom base is 16 nm, and the diameter of the top of the truncated hexagonal pyramid is 6 nm. The growth direction is along the (0001) direction. The geometry model in our simulation is shown in Fig.1.[7] The quantum dot is embedded in the AlN matrix, with a dimension of $30\times30\times30\text{nm}^3$, and the wetting layer is located at the centre of the growth axis.

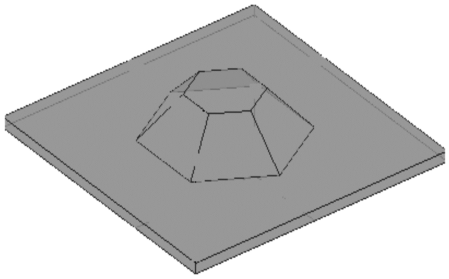


Fig.1. Schematic drawing of the truncated hexagonal pyramid shaped GaN/AlN quantum dot.

The distribution of strain is visualized in Fig.2, where ε_{xx}, ε_{yy}, ε_{zz}, and ε_{xz} are shown in the $(0\bar{1}10)$ plane through the centre of the quantum dot. From Fig.2, one can notice that the normal strain (ε_{xx}, ε_{yy}, ε_{zz}) distributions are symmetric about the z-axis, but the shear strain distributions (Fig.2(e)) are not symmetric about the z-axis. In Figs.2(a) and 2(b), the tensile strain occupies below and above the island, it can be noticed that the compress strain in the quantum dot relaxes from the initial value –0.024 to about –0.02. From Fig.2(c), the ε_{zz} strain distributions, due to the Poisson effect, show a compressive strain below and above the island, and in the island the initial compressive strain still larger than the Poisson effect induced tensile strain, so in the island there exists a compressive strain too. Figure 2(d) shows a biaxial strain distribution, which is related to the valence band edge. The biaxial is defined as $\varepsilon_{bi} = 2\varepsilon_{zz} - \varepsilon_{xx} - \varepsilon_{yy}$, where the subindex '*bi*' means biaxial. From Fig.2(e), the shear strain mainly concentrates in a boundary region between the quantum dot and the surrounding barriers, and in the other parts the shear strain quickly decreases to zero. Figure 2(f) shows a hydrostatic strain distribution, as can be seen, in the inside of the quantum dot, the hydrostatic strain value is almost constant, the hydrostatic strain value in the barrier region is near to zero. From the above regions of the quantum dot, one can see a tensile strain induced by the buried island. This also suggests that on the growth of a subsequent sheet of quantum dots, there appears a tendency for the islands to form in these regions: the formation of a cluster of atoms or a new island in the tensile strain region means the reduction of system strain energy.

Figure 3(a) shows the detailed strain distribution information along the (0001) direction through the centre of quantum dot. As can be seen in Fig.3(a), along the symmetric axis the ε_{xx} and the ε_{yy} strain components are equal, the ε_{zz} is the compressive strain along the symmetric axis, and the hydrostatic strain value is about –0.04. And these strain components are almost constant in the quantum dot region while they are zero in the surrounding barriers. All the strain components approach to zero in the region far from the quantum dot. Figures 3(b) and 3(c) show the strain distributions along the $(2\bar{1}\bar{1}0)$ and the $(0\bar{1}10)$ directions through the centre of the base, respectively. It can be further noticed that the shear strains concentrate only in the boundary between the quantum dot and the barriers. The maximum values of the strain are located in the corners of the quantum dot, which can also be seen in Fig.2.

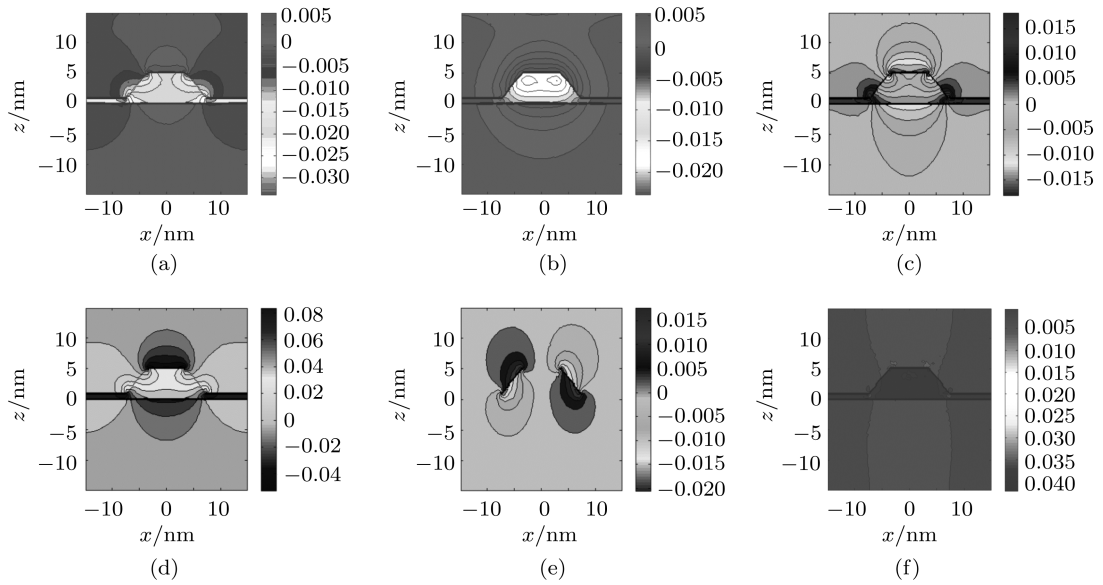


Fig.2. The strain distribution in the $(0\bar{1}10)$ plan through the centre of the quantum dot, where panels (a), (b), (c), (d), (e) and (f) are for ε_{xx}, ε_{yy}, ε_{zz}, $\varepsilon_{\rm bi}$, ε_{xz} and $\varepsilon_{\rm hyd}$ strain components respectively.

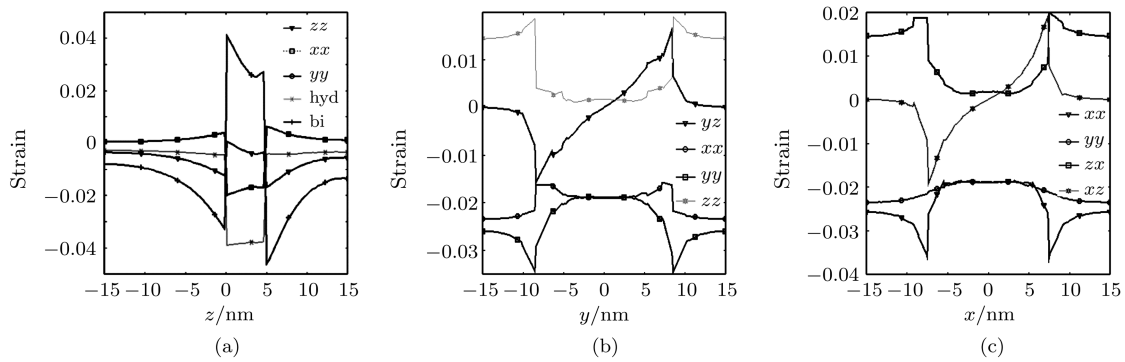


Fig.3. The different strain distributions along the z, y and x axes, where xx, yy, zz, hyd, bi, yz, and xz represent ε_{xx}, ε_{yy}, ε_{zz}, $\varepsilon_{\rm hyd}$, $\varepsilon_{\rm bi}\varepsilon_{yz}$, and ε_{xz} strain components respectively.

From Eq.(8), the strengths of the polarizations are related to not only the shear strain components (ε_{xz}, ε_{yz}) but also the normal strain components (ε_{xx}, $\varepsilon_{yy}, \varepsilon_{zz}$). The shear strain determines the components $P_x^{\rm strain}$ and $P_y^{\rm strain}$, and the normal strain determines the component $P_z^{\rm strain}$. The strain analysis in Fig.3 shows that the shear strain mainly accumulates near the boundary region between the quantum dot and the surrounding barriers. On the one hand, the value of the shear strain is smaller than the value of normal strain (see Figs.3(b) and 3(c)), on the other hand, the piezoelectric coefficient for the $P_z^{\rm strain}$ is larger than those of the other components. So the polarization strength mainly accumulates on the $P_z^{\rm strain}$ components.

Figure 4(c), 4(b), and 4(a) show the total polarization distribution, the spontaneous polarization distribution and strain induced piezoelectric polarization distribution respectively. As can be seen, the strain induced polarization is about one third of the total polarization in strength. The polarization distribution is dependent on the shape of quantum dot. It should be noticed that the piezoelectric potential is mainly distributed in a barrier region, which may be due to the fact that the piezoelectric coefficient in a barrier AlN region is twice as large as that in a quantum dot GaN region. Figure 4(d) indicates that the polarization electric field is mainly distributed in the GaN quantum dot and the wetting layer. Figure 4(e) shows the piezoelectric potential distribution along the (0001) direction, through the central axis of the quantum dot. The maximum potential is bout

1.5 V. The spontaneous and the strain induced potentials are also shown in the figure. Figure 4(f) shows the electric field distribution along the (0001) direction, and through the central axis of the quantum dot, and as can be seen in the quantum dot, there exists a strong built-in field on the order of 10^8V/m.[13]

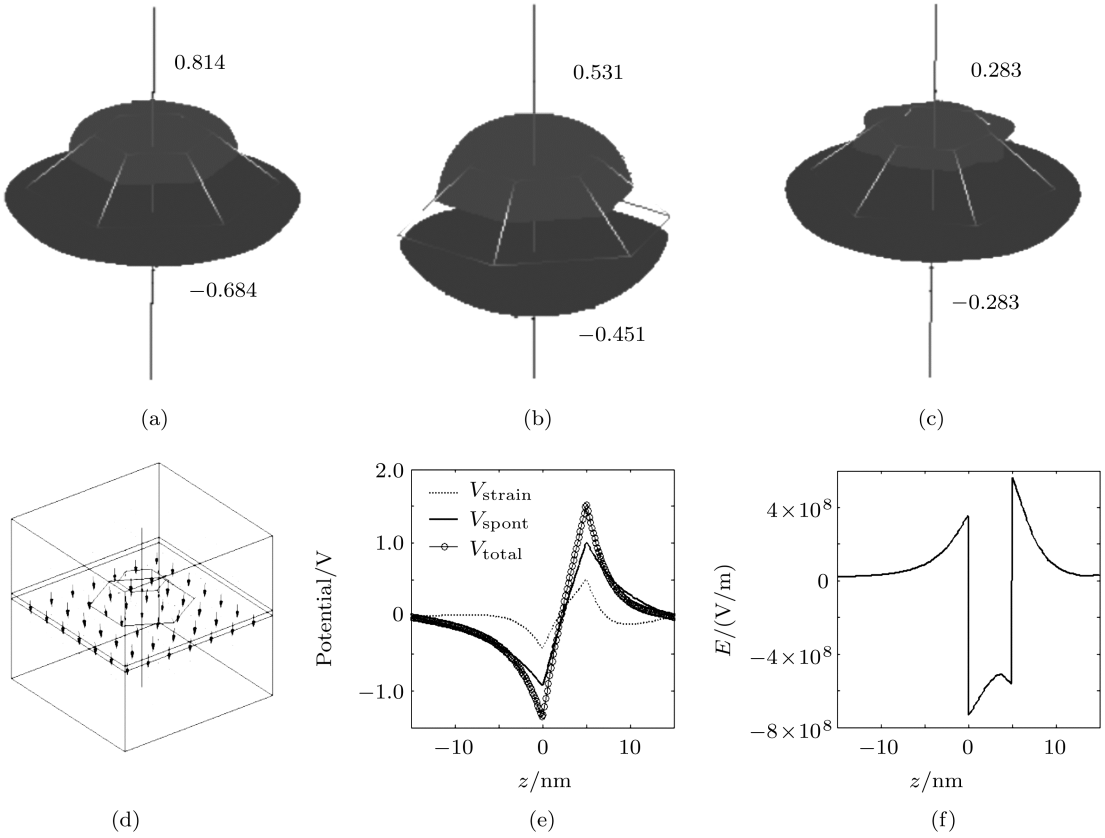


Fig.4. The iso-surface distribution of the piezoelectric polarization strengths, where panel (a) is for the total polarization, panel (b) for the spontaneous polarization, panel (c) for the strain induced polarization, panel (d) for the three-view of the built-in electric field, panels (e) and (f) for the polarization potential and built-in electric field distributions along the (0001) directions through the centre axis of the quantum dot, respectively.

The strain modified (conduction band, heavy-hole band) band edges and heavy hole valence band edges along the z axis are shown in Figs.5(a) and 5(b) respectively. As can be seen, the dominant effect of the strain is that in a dot region, there is a little increase in its band gap due to the hydrostatic strain. For example, the conduction band in the quantum dot raises its band edge from 3.475 to about 3.495 eV, which reduces the electron confinement in the well. So the main influence is due to the polarization effects. These effects greatly increase the barrier near the bottom of the quantum dot, and deepen the confinement potential near the upper part of the quantum dot. So the electron wavefunction is obviously localized near the upper part of the quantum dot. The valence band has a more complicated structure.[14,15] We only show the modified heavy hole band edge and will not further discuss it here. It is obvious that the hole wavefunction is localized near the bottom part of the quantum dot for its strong confinement to hole.

We now consider the computation of the electronic energy levels in a truncated hexagon pyramid shaped quantum dot. The bound states are determined by solving the Hamiltonian Eq.(12) numerically. The calculated energy levels for the ground state and the lowest four excited states in the conduction band are shown in Fig.6. The first ground state and the lowest four excited states energy levels are 3.002286, 3.097509, 3.0983, 3.20969, and 3.21021 eV, respectively. As can be seen, the wavefunctions are pushed up to the top part of the quantum dot, due to the polarization effect induced potential well confinement.

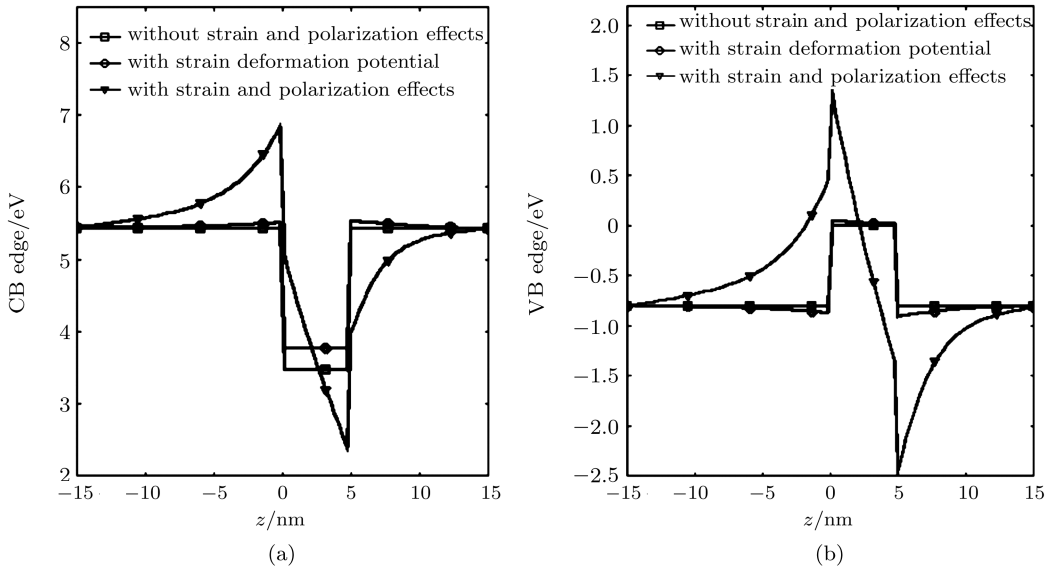


Fig.5. Strain and polarization modified conduction-band (CB) edges (a) and heavy hole valence band (VB) edges (b), where all the band edges are along the (0001) direction through quantum dot centre ($x = y = 0$).

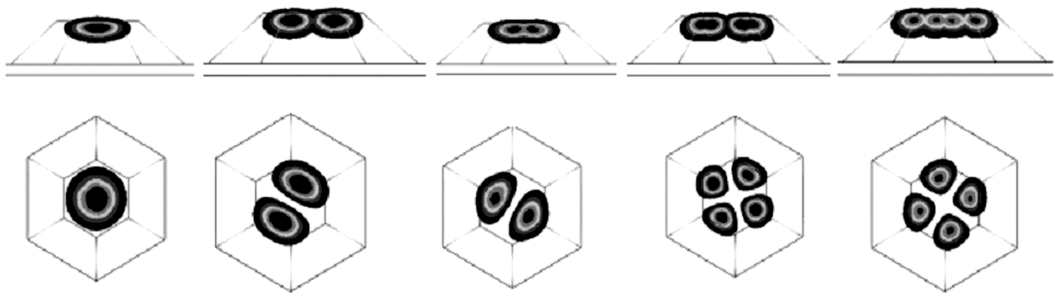


Fig.6. The three-dimensional views of electron probability density distributions for the five lowest bound states, where the upper part shows the side view from the $z - y$ plane, and the lower part indicates the side view from the $x - y$ plane.

7. Conclusions

The relaxation of the strain and its residual components in a self-organized GaN/AlN quantum dot are calculated by using the continuum elastic theory. As an example, we investigate a truncated hexagonal pyramid shaped quantum dots including a wetting layer. By taking into account the influence of the strain on the band gap and the piezoelectric potential, we solve a three-dimensional, effective mass single band Schrödinger equation for the electronic energy levels and wavefunctions. We find that our calculated results are in agreement with published results in the literature, so the theory analysis method and numerical technique used in this work are reasonable. The valuable information on the electronic structures is useful for the further study of optical transition rates and gain characteristics of materials. We expect these methods to be useful for analysing the semiconductor quantum electronics or optoelectronic devices, especially those strain heterostructure related semiconductor materials, such as GaN/AlN and InAs/GaAs. For applications of quantum electronics devices used to realize quantum information operations, the multibody effects should be taken into considerations. The Hartree–Fock approximation or the density function theory, other than single particle Eq.(12) should be used to calculate the electronic structure. These topics are beyond the scope of our present work.

References

[1] Stephanie M R and Manninen M 2002 *Rev. Mod. Phys.* **74** 1283

[2] Li S S, Xia J B, Yuan Z L and Xu Z Y 1996 *Phys. Rev.* B **54** 11575

[3] Li S S, Chang K and Xia J B 2005 *Phys. Rev.* B **71** 155301

[4] Liu Y M, Yu Z Y and Huang Y Z 2006 *Acta Phys. Sin.* **55** 5023 (in Chinese)

[5] Shi J J, Xia C X, Wei S Y and Liu Z X 2005 *J. Appl. Phys.* **97** 083705

[6] Vurgaftman I and Meyer J R 2003 *J. Appl. Phys.* **94** 3675

[7] Liu Y M, Yu Z Y and Huang Y Z 2007 *J. University Sci. Technol. Beijing* **14** 477

[8] Liu Y M, Yu, Z Y and Huang Y Z 2006 *Int. J. Modern Phys.* B **20** 4899

[9] Liu Y M, Yu, Z Y and Ren X M 2008 *Chin. Phys. Lett.* **25** 1850

[10] Pryor C, Wang L W, Williamson A J and Zunger A 1998 *J. Appl. Phys.* **83** 2548

[11] Moghraby D E, Johnson R G and Harrison P 2003 *Comput. Phys. Commun.* **155** 236

[12] Vladimir A F, Evghenii P P and Alexander A B 2003 *J. Nano. Sci. Nanotech.* **3** 253

[13] Siter O, Grundmann M and Bimberg D 1999 *Phys. Rev.* B **59** 5688

[14] Califano M and Harrison P 2002 *J. Appl. Phys.* **91** 389

[15] Shin H, Lee W and Yo H Y 2003 *J. Phys. Condens. Matter* **15** 3689